Structure of the *Pseudomonas aeruginosa* transamidosome reveals unique aspects of bacterial tRNA-dependent asparagine biosynthesis

Tateki Suzuki[a], Akiyoshi Nakamura[b,c], Koji Kato[b], Dieter Söll[c,1], Isao Tanaka[b], Kelly Sheppard[d], and Min Yao[a,b,1]

[a]Graduate School of Life Science and [b]Faculty of Advanced Life Science, Hokkaido University, Sapporo 060-0810, Japan; [c]Department of Molecular Biophysics and Biochemistry and Department of Chemistry, Yale University, New Haven, CT 06520; and [d]Department of Chemistry, Skidmore College, Saratoga Springs, NY 12866

Contributed by Dieter Söll, December 5, 2014 (sent for review November 11, 2014; reviewed by Adrian R. Ferré-D'Amaré)

Many prokaryotes lack a tRNA synthetase to attach asparagine to its cognate $tRNA^{Asn}$, and instead synthesize asparagine from $tRNA^{Asn}$-bound aspartate. This conversion involves two enzymes: a nondiscriminating aspartyl-tRNA synthetase (ND-AspRS) that forms Asp-$tRNA^{Asn}$, and a heterotrimeric amidotransferase GatCAB that amidates Asp-$tRNA^{Asn}$ to form Asn-$tRNA^{Asn}$ for use in protein synthesis. ND-AspRS, GatCAB, and $tRNA^{Asn}$ may assemble in an ∼400-kDa complex, known as the Asn-transamidosome, which couples the two steps of asparagine biosynthesis in space and time to yield Asn-$tRNA^{Asn}$. We report the 3.7-Å resolution crystal structure of the *Pseudomonas aeruginosa* Asn-transamidosome, which represents the most common machinery for asparagine biosynthesis in bacteria. We show that, in contrast to a previously described archaeal-type transamidosome, a bacteria-specific GAD domain of ND-AspRS provokes a principally new architecture of the complex. Both $tRNA^{Asn}$ molecules in the transamidosome simultaneously serve as substrates and scaffolds for the complex assembly. This architecture rationalizes an elevated dynamic and a greater turnover of ND-AspRS within bacterial-type transamidosomes, and possibly may explain a different evolutionary pathway of GatCAB in organisms with bacterial-type vs. archaeal-type Asn-transamidosomes. Importantly, because the two-step pathway for Asn-$tRNA^{Asn}$ formation evolutionarily preceded the direct attachment of Asn to $tRNA^{Asn}$, our structure also may reflect the mechanism by which asparagine was initially added to the genetic code.

transamidosome | asparagine biosynthesis | aspartyl-tRNA synthetase | GatCAB

Accurate translation of the genetic code into a protein sequence relies on a covalent attachment of amino acids to cognate tRNAs that are later used in protein synthesis (1). This attachment is catalyzed by aminoacyl-tRNA synthetases (aaRSs), each specific to one amino acid and a set of tRNA isoacceptors (2). However, the majority of prokaryotes lack several tRNA synthetases, particularly asparaginyl-tRNA synthetase (AsnRS), which ligates asparagine to $tRNA^{Asn}$ (3, 4). In these organisms, asparagine is synthesized in a two-step, tRNA-dependent pathway (5). First, a nondiscriminating aspartyl-tRNA synthetase (ND-AspRS) attaches aspartate to $tRNA^{Asn}$ to form Asp-$tRNA^{Asn}$ (6, 7). Then the tRNA-bound aspartate is converted to asparagine by the amidotransferase (AdT) GatCAB to yield the final product, Asn-$tRNA^{Asn}$ (6, 8–13). Likewise, in prokaryotes lacking glutaminyl-tRNA synthetase (GlnRS), Gln-$tRNA^{Gln}$ is formed by the sequential actions of a nondiscriminating glutamyl-tRNA synthetase (ND-GluRS) (14) and an AdT (5). In bacteria, the role of AdT is played by GatCAB (15), whereas in archaea, it is played by GatDE (16, 17).

More than 25 years ago (18), it was proposed that ND-aaRSs and AdTs may form a complex—now called a transamidosome—to couple the two steps of Asn-$tRNA^{Asn}$ formation in space and time and allow efficient transfer of Asp-$tRNA^{Asn}$ from the aaRS to the AdT. The first characterized transamidosome was the Asn-transamidosome from *Thermus thermophilus* (*Tt*Asn-transamidosome) (19, 20). This complex was identified as a tRNA-dependent association of AspRS2 (*Tt*AspRS2) and GatCAB in a 2:2:2 ratio. It was shown that transamidosome formation stabilizes interactions between subunits of GatCAB (21) and protects Asn-$tRNA^{Asn}$ from hydrolysis, with product release being rate-limiting (19). In the complex, the AspRS forms a dimer with only one catalytic site active at a time (21). It was suggested that the key advantages of asparagine formation by the transamidosome compared with separate enzymes are enhanced aspartylation of $tRNA^{Asn}$ and better prevention of the misacylated Asp-$tRNA^{Asn}$ from use in translation, because this would compromise the fidelity of protein synthesis (19–21).

Importantly, *Tt*AspRS2 was acquired through horizontal gene transfer from archaea (10), and lacks the GAD domain typical of bacterial AspRSs (22). The *Tt*Asn-transamidosome crystal structure suggests that a complex between bacterial ND-AspRS and GatCAB should be less stable and more structurally distinct than the *T. thermophilus* complex, owing to the presence of the GAD domain in bacterial ND-AspRS (21, 23). Consistent with this notion, the stable association of the *Helicobacter pylori* ND-AspRS (*Hp*ND-AspRS) with GatCAB requires the presence of an auxiliary factor, Hp0100 (23, 24). In the complex, the activity of the *Hp*ND-AspRS is unchanged, although the activity of GatCAB increases (23); however, Hp0100 is phylogenetically limited to ε-proteobacteria (23). Therefore, most bacteria have

Significance

The present structure reveals the architecture of the *Pseudomonas aeruginosa* bacterial-type asparagine-transamidosome, the most common macromolecular assembly required for asparaginyl-$tRNA^{Asn}$ formation in bacteria. We show that the presence of an additional GAD domain in the aspartyl-tRNA synthetase, common in most bacteria but missing in the archaeal-type *Thermus thermophilus* transamidosome, results in a complex with a distinct architecture and stoichiometry. Furthermore, our kinetic studies reveal that bacterial transamidosomes have distinct kinetic properties compared with the archaeal complex, with rapid release of the Asn-$tRNA^{Asn}$ product, leading to improved turnover by the bacterial-type aspartyl-tRNA synthetase in the complex. Overall, our study provides a structural basis for understanding tRNA-dependent asparagine biosynthesis found in the in majority of bacterial species.

Author contributions: T.S., A.N., D.S., I.T., K.S., and M.Y. designed research; T.S., A.N., and K.S. performed research; T.S., A.N., K.K., D.S., I.T., K.S., and M.Y. analyzed data; and T.S., A.N., D.S., K.S., and M.Y. wrote the paper.

Reviewers included: A.R.F.-D., National Heart, Lung, and Blood Institute, NIH.

The authors declare no conflict of interest.

Data deposition: The atomic coordinates and structure factors have been deposited in the Protein Data Bank, www.pdb.org (PDB ID codes 4WJ4 and 4WJ3).

[1]To whom correspondence may be addressed. Email: dieter.soll@yale.edu or yao@castor.sci.hokudai.ac.jp.

This article contains supporting information online at www.pnas.org/lookup/suppl/doi:10.1073/pnas.1423314112/-/DCSupplemental.

a structurally and, possibly, functionally distinct class of transamidosomes than those described by the *T. thermophilus and H. pylori* complexes.

In the bacterium *Pseudomonas aeruginosa*, Asn-tRNA^{Asn} formation is catalyzed by GatCAB and bacterial ND-AspRS, and thus represents the most common type of bacterial Asn-transamidosome (25). Here we report the crystal structure of the *P. aeruginosa* Asn-transamidosome (*Pa*Asn-transamidosome), which represents the transamidation state of the Asn-tRNA^{Asn} formation. The structure suggests that the additional GAD domain within the ND-AspRS changes the overall architecture of the complex relative to the previously described *Tt*Asn-transamidosome. Consistent with the structure, our in vitro measurements show that *Pa*Asn-transamidosome has unique kinetic properties and functions primarily to enhance tRNA^{Asn} turnover and facilitate Asp-tRNA^{Asn} handoff from AspRS to GatCAB.

Results

Overall Structure of the Bacterial Asn-Transamidosome. The structure of the *Pa*Asn-transamidosome determined at 3.7-Å resolution (Table S1) reveals the architecture of a 413-kDa symmetric complex comprising ND-AspRS, GatCAB, and tRNA^{Asn} in a 2:2:2 stoichiometry. Each GatCAB is bound to a different tRNA^{Asn} and ND-AspRS, and all are related by a noncrystallographic twofold axis at the interface of the ND-AspRS monomers (Fig. 1*A*). The complex is stably formed without the auxiliary factor Hp0100 (Fig. S1), although an association of ND-AspRS with GatCAB is tRNA-dependent, as described previously (19, 24). Consistent with the crystal structure, an ∼400-kDa complex was detected in solution by gel filtration (Fig. S2).

The structure reveals the interface between ND-AspRS and GatCAB. The α3 helix and β-hairpin connecting β-strands 13 and 14 in GatB contacts the C-terminal loop of ND-AspRS with an average interaction surface of ∼553 Å^2 (Fig. 1*B*, Fig. S3*A*, and Table S2). In addition, Arg583 and Arg585 in ND-AspRS are in a salt bridge distance from Glu236, Glu239, and Asp240 in GatB and seem to further stabilize the complex. Notably, these residues are largely conserved in organisms that use GatCAB (Fig. S4*A*) with a ND-AspRS (Fig. S4*B*), suggesting a common mode of GatB–ND-AspRS interaction across bacterial species.

The two tRNA^{Asn} molecules are bound to the complex in an identical manner (Fig. 1*C*). The ND-AspRS anticodon-binding domain (ABD) recognizes the anticodon of the tRNA, whereas the 3′ CCA terminus of tRNA^{Asn} is accommodated by the active site of GatCAB with the tRNA^{Asn} U1-A72 base pair near the 3_{10} turn in the GatB cradle domain. Consistent with previous studies, recognition of the U1-A72 base pair by the 3_{10} turn enables the bacterial AdT to distinguish its tRNA substrates (tRNA^{Asn} and tRNA^{Gln}) from tRNA^{Asp} and tRNA^{Glu} (21, 26–28). As seen in the *Staphylococcus aureus* GatCAB structure (27), the tail domain of GatB is positioned to size the D-loop of the tRNA, another major tRNA recognition element of bacterial GatCAB (26, 28). Accordingly, the structure likely represents the transamidation state of the bacterial Asn-transamidosome.

Unique Structural Features of the Bacterial Asn-Transamidosome. The key difference between bacterial and archaeal-type transamidosomes is the presence of an additional GAD domain in the ND-AspRS proteins. The structural superposition of the *Pa*Asn-transamidosome with the *Tt*Asn-transamidosome (21) reveals how the GAD domain alters the overall architecture of the bacterial complex.

The previously described *Tt*Asn-transamidosome comprises two dimers of the archaeal type *Tt*AspRS2, two GatCABs, and four tRNA^{Asn} molecules, although one *Tt*AspRS2 dimer seems to dissociate from the complex in solution, according to small angle X-ray scattering analysis (21). The structure likely represents a transitional step in Asn-tRNA^{Asn} formation. It was initially proposed that tRNA-dependent Asn biosynthesis in *T. thermophilus* requires binding of two tRNA molecules to the *Tt*AspRS2 dimer (21). Two GatCAB molecules are then recruited and induce conformational changes in the *Tt*AspRS2 dimer in such a way that makes only one *Tt*AspRS2 monomer active at a time. In this complex, one tRNA molecule ($_{cat}$tRNA^{Asn}) is bound to the active *Tt*AspRS2 monomer to be aspartylated (Fig. 2*A*), whereas the other tRNA molecule ($_{scaf}$tRNA^{Asn}) binds to the inactive monomer and plays the role of a scaffold that stabilizes the complex. In agreement with the structure, *Tt*AspRS2 activity in the *Tt*Asn-transamidosome has biphasic kinetics, with only one-half of the catalytic sites active at a time (19, 21).

We show that, unlike the *Tt*Asn-transamidosome, the *Pa*Asn-transamidosome comprises only one ND-AspRS dimer bound to two tRNA^{Asn} molecules and two GatCAB molecules (Fig. 1*A*). Both tRNA molecules adopt a uniform $_{cat}$tRNA^{Asn} conformation, suggesting that both ND-AspRS monomers can be active at the same time. The differences between the two Asn-transamidosomes likely are related to the bacteria-specific GAD insertion domain. Superposition of the ND-AspRS in the *Pa*Asn-transamidosome and *Tt*Asn-transamidosome reveals a steric clash between the GAD domain of the *Pa*ND-AspRS and the *Tt*GatCAB (Fig. 2*B*). In the *Pa*Asn-transamidosome, the *Pa*GatCAB bends away from the rest of the complex to accommodate the *Pa*ND-AspRS GAD domain. This particular orientation of GatCAB in the *Pa*Asn-transamidosome enables both tRNA^{Asn} molecules bound to the ND-AspRS dimer to adopt $_{cat}$tRNA^{Asn} conformations.

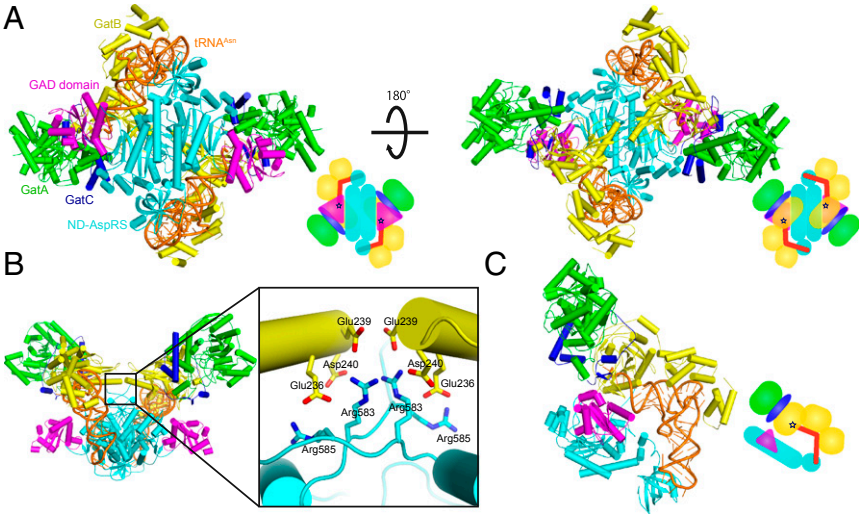

Fig. 1. (*A*) Overall structure of the Asn-transamidosome from *P. aeruginosa*. The catalytic and ABDs of ND-AspRS are shown in cyan, the insertion domain characteristic of bacterial AspRS (GAD domain) is in magenta, GatC is in blue, GatA is in green, GatB is in yellow, and tRNA^{Asn} is in orange. The 3′ terminus of tRNA^{Asn} positioned in the active site of GatB is represented by a dark-blue star in the schematic diagram. (*B*) Close-up view of the GatB and ND-AspRS interface region. The acidic and basic residues clustered around the interface region are shown as stick models. (*C*) A catalytic unit (one ND-AspRS, one GatCAB, and one tRNA^{Asn}) of the *Pa*Asn-transamidosome.

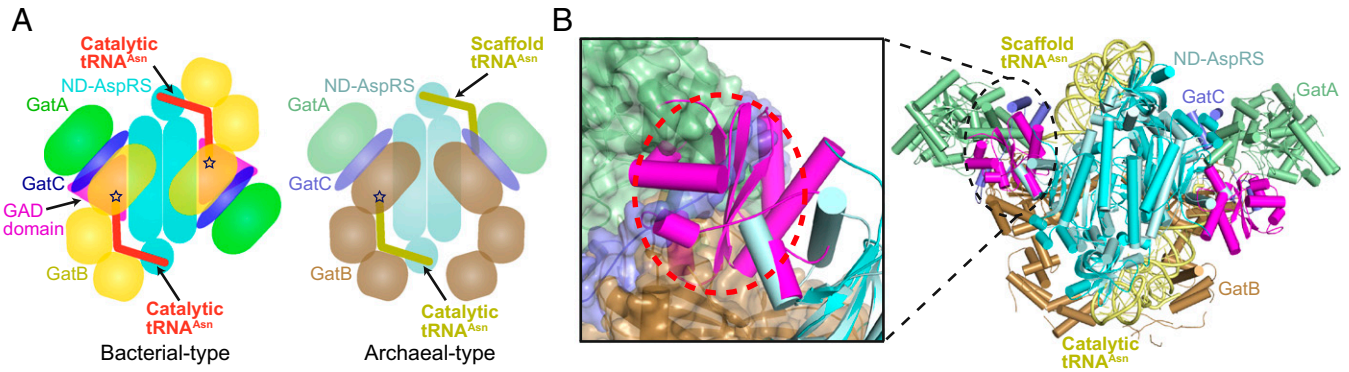

Fig. 2. (*A*) Schematic comparison of the *Pa*Asn-transamidosome (bacterial type) with the *Tt*Asn-transamidosome (archaeal type) highlighting different architectures and tRNA-binding modes. The 3′ terminus of $tRNA^{Asn}$ positioned in the active site of GatB is represented by a dark-blue star in the schematic diagram. (*B*) Superposition of the ND-AspRS in the *Pa*Asn-transamidosome on that in the *Tt*Asn-transamidosome. (*Left*) Close-up view of the GatCAB-bound scaffold $tRNA^{Asn}$ in the *Tt*Asn-transamidosome, represented as a surface model, and the GAD domain of the ND-AspRS in the *Pa*Asn-transamidosome. The steric clash between the GAD domain of ND-AspRS in the *Pa*Asn-transamidosome and the GatCAB bound scaffold $tRNA^{Asn}$ in the *Tt*Asn-transamidosome is represented by a red dotted circle. The structure of the *Tt*Asn-transamidosome is rotated 180° from *A* along the axis parallel to the paper surface.

The lack of a GAD insertion in the *Tt*AspRS2 allows the *Tt*GatCAB to bend toward the catalytic core of *Tt*AspRS2, facilitating the binding of one $tRNA^{Asn}$ in the $_{scaf}tRNA^{Asn}$ confirmation (21).

Distinct Biochemical Properties of the Bacterial Asn-Transamidosome. To test whether a distinct architecture of the complex results in distinct kinetic properties, we measured how the *Pa*Asn-transamidosome protects Asn-$tRNA^{Asn}$ from hydrolysis. The lack of $_{scaf}tRNA^{Asn}$ to stabilize the complex suggests that the *Pa*Asn-transamidosome can readily release Asn-$tRNA^{Asn}$ after product formation. Our measurements show that, consistent with that hypothesis and unlike the *Tt*Asn-transamidosome, the *P. aeruginosa* complex does not protect Asn-$tRNA^{Asn}$ from deacylation ($t_{1/2}$ of 29 min vs. 29 min with just GatCAB present). In a similar manner, the *Pa*Asn-transamidosome does not protect Asp-$tRNA^{Asn}$ from hydrolysis better than GatCAB alone ($t_{1/2}$ of 238 min and 246 min, respectively). However, *Pa*GatCAB does protect Asp-$tRNA^{Asn}$ from deacylation ($t_{1/2}$ of 246 min vs. 39 min with no enzyme present and 41 min with ND-AspRS present), but offers minimal protection of Asn-$tRNA^{Asn}$ ($t_{1/2}$ of 29 min vs. 22 min without enzyme), consistent with GatCAB binding Asp-$tRNA^{Asn}$ to generate and release Asn-$tRNA^{Asn}$ for protein synthesis.

In agreement with the results of the protection assay, we did not detect burst phase kinetics with the *Pa*Asn-transamidosome that had been observed with the *Tt*Asn-transamidsome (19, 21). The association of GatCAB with ND-AspRS did increase ND-AspRS turnover by 3.2-fold; however, the presence of GatCAB also increased the K_m of ND-AspRS for $tRNA^{Asn}$ by a similar factor, leading to no difference in ND-AspRS catalytic efficiency (Table 1). Taken together, the kinetic data show that the *Pa*Asn-transamidosome can readily release Asn-$tRNA^{Asn}$ after its formation. This biochemical property may be a reflection of the GAD insertion rather than the lack of $_{scaf}tRNA^{Asn}$ to stabilize the complex.

We attempted to determine whether the bacterial Asn-transamidosome can behave like the archaeal Asn-transamidsome when the GAD insertion domain is deleted. Unfortunately, none of the *Pa*ND-AspRS deletion mutant constructs (including a replacement of the GAD domain with the loop found in *Tt*AspRS2) produced sufficient protein amounts for analysis.

Structural Basis of the CCA Terminus Translocation During the Transamidation Cycle. The *Pa*Asn-transamidosome structure likely represents the transamidation state of the complex; thus, we determined the cocrystal structure of *Pa*ND-AspRS with $tRNA^{Asn}$ at 3.3-Å resolution to provide insight into the aminoacylation state of *Pa*ND-AspRS with $tRNA^{Asn}$ (Fig. 3 *A* and *B* and Table S1). Overall, the *Pa*ND-AspRS:$tRNA^{Asn}$ binary complex is similar to the *Escherichia coli* D-AspRS (*Ec*D-AspRS) enzyme bound to $tRNA^{Asp}$ (PDB ID code 1C0A) (29) and reveals subtle differences in the tRNA structures that may explain tRNA specificity of the enzyme (*SI Text* and Figs. S5–S7).

The 3′ CCA ends of both $tRNA^{Asn}$ molecules bound to the *Pa*Asn-transamidosome are positioned at the GatCAB transamidase active site. However, for tRNA-dependent Asn biosynthesis, the tRNA first must be aspartylated by ND-AspRS. Thus, the 3′ end must bind in the ND-AspRS active site and then flip ~40 Å up into the GatCAB catalytic site after Asp-$tRNA^{Asn}$ formation. To clarify how the ND-AspRS accommodates the shifting of the CCA $tRNA^{Asn}$ terminus, we superposed the *Pa*ND-AspRS bound to $tRNA^{Asn}$ onto that in the *Pa*Asn-transamidosome, with respect to the ABD (Fig. 4*A*). This superposition revealed that when the tRNA acceptor end flips from the active site of ND-AspRS to GatCAB, the catalytic domain shifts backward away from the tRNA. The shift is possible because of a hinge between the ABD and catalytic domain of ND-AspRS. In addition, the GAD insertion and helix bundle appends to the catalytic domain shift to open up the *Pa*ND-AspRS catalytic site (Fig. 4*B*). Presumably, this movement facilitates the flipping of the tRNA acceptor stem from ND-AspRS to GatCAB.

These structural rearrangements in the ND-AspRS are accompanied by an ~14-Å shift of the $tRNA^{Asn}$ elbow and an ~40-Å

Table 1. Kinetic data for Asp-$tRNA^{Asn}$ formation by *P. aeruginosa* ND-AspRS

Enzyme	K_M, μM, mean ± SD	k_{cat}, s^{-1}, mean ± SD	k_{cat}/K_M, s^{-1}/μM, mean ± SD
AspRS	0.61 ± 0.07	0.111 ± 0.006	0.18 ± 0.02
AspRS + GatCAB*	2.0 ± 0.2	0.36 ± 0.01	0.18 ± 0.02

Measurements are from three separate experiments. Reactions with *P. aeruginosa* ND-AspRS (5 nM) were carried out at 37 °C in the presence of excess ATP (4 mM), Asp (3.3 mM), and Gln (2 mM), as described in *Materials and Methods*. The concentration of $tRNA^{Asn}$ varied between 0.1 and 10.1 μM.
*GatCAB (2.0 μM) was added to the reaction mixture.

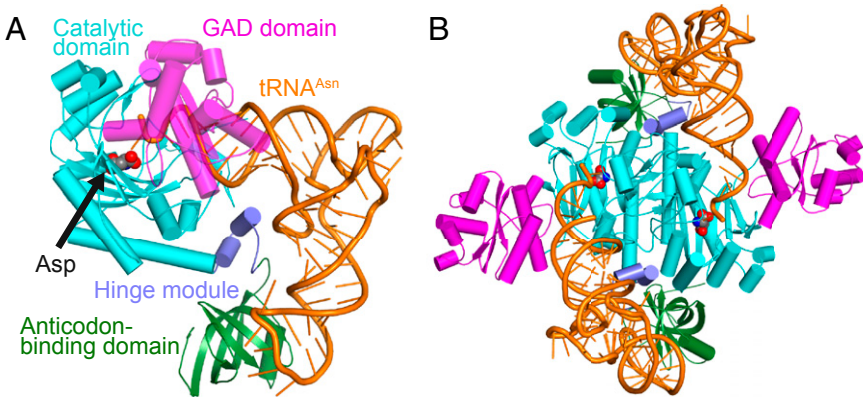

Fig. 3. (*A*) Monomeric structure of the *P. aeruginosa* ND-AspRS:tRNA^{Asn} (*Pa*ND-AspRS:tRNA^{Asn}) binary complex in an asymmetric unit. The ABD (green), catalytic domain (cyan), GAD domain (magenta), and hinge region (blue) of the ND-AspRS are shown with tRNA^{Asn} (orange). ND-AspRS-bound Asp is shown as a sphere model. (*B*) Dimeric structure of the *Pa*ND-AspRS:tRNA^{Asn} binary complex. Each monomer is related by a crystallographic twofold axis.

movement of the tRNA^{Asn} 3′ CCA end during the transition from the aminoacylation to transamidase state (Fig. 4*C*). Superposition of the T-arms of the tRNA in the two states revealed rearrangements within the tRNA^{Asn} D-loop (Fig. 4*D* and Fig. S3 *B* and *C*). The shift results in C17 being flipped out of the D-loop and U20 pointing down toward the anticodon instead of up toward the TΨC-loop. Accordingly, G18 is shifted so it no longer hydrogen-bonds with U55. Similar structural changes are seen in the GatDE-tRNA^{Gln} structure (17).

Bacterial Asn-Transamidosome Structure Reveals the GatCAB Transamidation State. With the tRNA^{Asn} 3′ end bound in the GatCAB active site, the *Pa*Asn-transamidosome likely represents the transamidation state of the complex. Apart from association with ND-AspRS, bacterial GatCAB can form a ternary complex with ND-GluRS and tRNA^{Gln}, known as a Gln-transamidosome and typical of organisms lacking a GlnRS (30, 31). In the *Thermotoga maritima* (*Tm*) Gln-transamidosome structure (30), the tRNA^{Gln} 3′ end is bound in the GluRS active site, and the GatCAB tail domain is associated with the D-loop of the tRNA. The structure likely represents the aminoacylation state of the bacterial GatCAB in a transamidosome.

To reveal the structural differences between GatCAB in the aminoacylation and transamidation states, we superposed GatB in the *Pa*Asn-transamidosome with the subunit in the *Tm*Gln-transamidosome (30) and the unbound *S. aureus* GatCAB structure (27, 28) with respect to the GatB helical domain. As was seen in the *Tm*Gln-transamidosome (30), we found two hinge regions in the *Pa*GatB, between the helical domain and the cradle and tail domains (Fig. 5). In both transamidosomes, the GatB tail domain is curled toward the GatB helical and cradle domains compared with the unbound structure, enabling the AdT subunit to bind to the tRNA D-loop. The movement is facilitated by the flexibility of the hinge between the helical and tail domains. In the *Tm*Gln-transamidosome, the GatB cradle domain is turned up away from the other two domains to facilitate binding of the acceptor stem of the tRNA in the GluRS active site (30). Similar positioning by the *Pa*GatB would help accommodate the tRNA^{Asn} 3′ end bound in the ND-AspRS active site (Fig. 3*A*). In the transamidation state of the *Pa*Asn-transamidosome, the GatB cradle domain is curled toward the helical domain, although not to the same extent as the unbound GatCAB. The positioning allows GatB to bind the tRNA acceptor stem.

Discussion

Complexes of Translation Components for Improved Protein Synthesis. Multi-aaRS complexes, or complexes of aaRSs with other translation machinery components, are known in all domains of life (32). Such higher-order structures have been shown to contribute to translational fidelity and to increased catalytic efficiency of aaRS reactions (33–35). The allure of substrate channeling (36), preventing the participation of misacylated aminoacyl-tRNA in protein synthesis, led to the suggestion of a multienzyme complex for tRNA-dependent Gln-tRNA synthesis (18). This has been borne out by detailed analyses of Gln-tRNA and Asn-tRNA formation by transamidosomes in bacteria and archaea (this work and refs. 19 and 30), although exceptions might exist (37). The transamidosome architecture nicely explains substrate channeling and efficient aa-tRNA formation by the transamidation route. Another multimeric complex (consisting of SepRS, SepCysS,

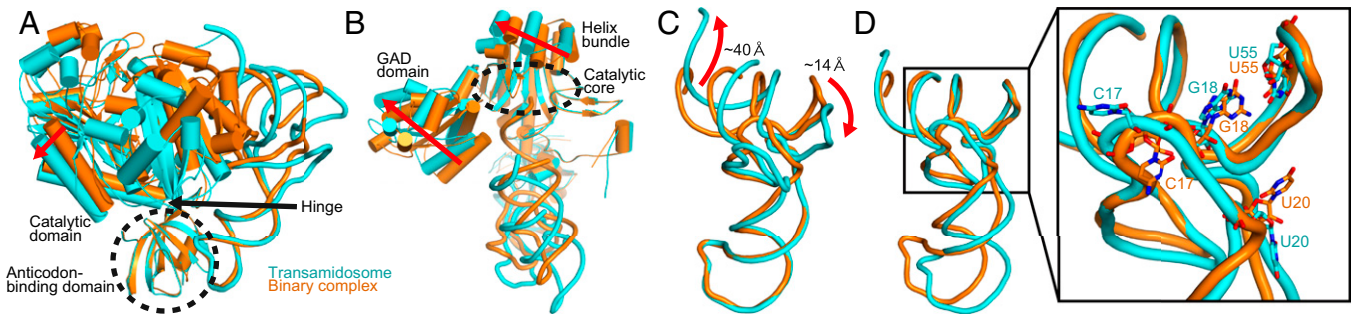

Fig. 4. (*A*) Superposition of the *Pa*ND-AspRS:tRNA^{Asn} structure in the binary complex onto that in the *Pa*Asn-transamidosome with respect to the ABD. The black dotted circle represents the ABD, and the red arrow denotes the shift of the catalytic domain from the binary complex to the transamidosome. (*B*) Superposition of the *Pa*ND-AspRS:tRNA^{Asn} binary complex on that in the *Pa*Asn-transamidosome with respect to the catalytic core. The black dotted circle represents the catalytic core, and the red arrow denotes the shift of the GAD domain and helix bundle from the binary complex to the transamidosome. (*C*) Superposition of the tRNA^{Asn} structure in the binary complex on that in the *Pa*Asn-transamidosome with respect to the anticodon arm. The red arrow denotes the shift of the acceptor, D-arm, and T-arm from the binary complex to the transamidosome. (*D*) Superposition of the tRNA^{Asn} structure in the binary complex onto that in the *Pa*Asn-transamidosome with respect to the T-arms. Structurally different nucleotides between tRNA^{Asn} in the binary complex and the Asn-transamidosome are shown as stick models.

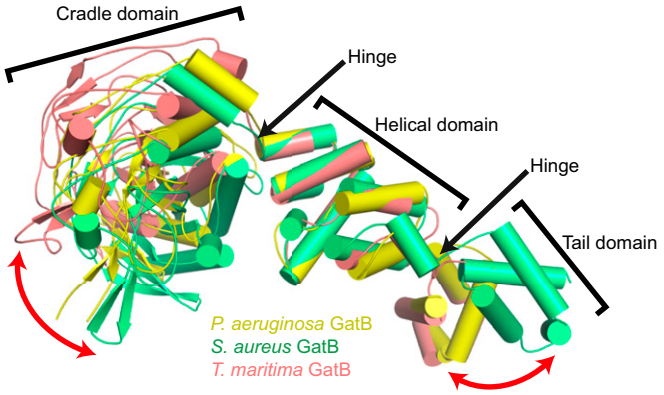

Fig. 5. Superposition of three GatB structures from *P. aeruginosa* (yellow), *S. aureus* (PDB ID code 3IP4; green), and *T. maritima* (PDB ID code 3ALO; pink) with respect to the helical domain showing two hinges in each domain interface. The movements of the cradle and tail domains are indicated by red arrows.

SepCysE, and $tRNA^{Cys}$) is essential for Cys-tRNA formation in methanogens (38). It is likely that the tRNA-dependent selenocysteine pathway also may involve a complex of $tRNA^{Sec}$, SerRS, PSTK, and SepSecS (39).

Bacterial tRNA-Dependent Asn Biosynthesis. Taken together, our data suggest that tRNA-dependent Asn biosynthesis in bacteria (Fig. 6) is overall analogous to Gln-$tRNA^{Gln}$ formation by the *Tm*Gln-transamidosome (30). At the initial step, the *Pa*ND-AspRS binds $tRNA^{Asn}$ with its anticodon positioned in the enzyme's binding domain and the $tRNA^{Asn}$ 3′ end positioned in the enzyme's active site, as seen in the cocrystal structure of *Pa*ND-AspRS complexed with $tRNA^{Asn}$. The GatB tail domain binds the tRNA's D-loop to distinguish $tRNA^{Asn}$ from $tRNA^{Asp}$, with the GatB cradle domain turned away from the complex to accommodate the tRNA acceptor stem bound in the ND-AspRS active site, as observed in the *Tm*Gln-transamidosome aminoacylation state (Fig. 6*A*). Aspartylation of the 3′-CCA terminus of $tRNA^{Asn}$ occurs in the aminoacylation state of the bacterial Asn-transamidosome. Asp-$tRNA^{Asn}$ formation triggers a conformational shift of the ND-AspRS GAD insertion and that catalytic domain and helix bundle appended to the catalytic domain. By opening up the ND-AspRS active site, this intermediate state facilitates the dissociation of the tRNA acceptor stem from ND-AspRS and a flipping up toward GatCAB (Fig. 6*B*). Finally, GatCAB, in particular the GatB cradle domain, moves into position to bind the $tRNA^{Asn}$ acceptor stem and adopt the transamidation state seen in the *Pa*Asn-transamidosome crystal structure (Fig. 6*C*). The 3_{10} turn in the GatB cradle domain selectively binds the $tRNA^{Asn}$ U1-A72 base pair; this provides a second check to ensure that Asp-$tRNA^{Asn}$ is amidated and not Asp-$tRNA^{Asp}$ (21, 26–28).

Now the $tRNA^{Asn}$-bound Asp is positioned in the GatCAB transamidase active site for amidation. Following Asn-$tRNA^{Asn}$ production, the complex dissociates, releasing Asn-$tRNA^{Asn}$, consistent with the complex's inability to protect Asn-$tRNA^{Asn}$ from hydrolysis. Given that the association of the *Pa*GatCAB and *Pa*ND-AspRS is tRNA-dependent, GatCAB is also likely released from ND-AspRS when Asn-$tRNA^{Asn}$ dissociates.

Evolution of Asn-Transamidosomes. In archaea, GatCAB is used only for Asn-$tRNA^{Asn}$ formation as GatDE forms Gln-$tRNA^{Gln}$ (16, 17). Both AdTs likely were present in early archaea (40). The specificity of archaeal GatCAB for Asn-$tRNA^{Asn}$ synthesis might have enabled archaeal AspRS to coevolve with the AdT to form a thermostable complex in which GatCAB is not released following Asn-$tRNA^{Asn}$ synthesis. This stability likely was facilitated by the archaeal AspRS not retaining the GAD insertion domain found in bacterial-type AspRS. The thermostability of the archaeal complex may explain why *T. thermophilus* acquired an archaeal-type AspRS for tRNA-dependent Asn biosynthesis instead of using the bacterial-type AspRS that it also encodes in its genome (19, 21, 22, 41).

Early bacteria likely emerged from the last universal common ancestral state (LUCAS) with just one AdT—GatCAB—for both Gln-$tRNA^{Gln}$ and Asn-$tRNA^{Asn}$ formation (40). After Asn-$tRNA^{Asn}$ formation in early bacteria, the release of GatCAB from bacterial ND-AspRS might be have been beneficial, because the free GatCAB could easily be repurposed for Gln-$tRNA^{Gln}$ formation with GluRS. In that context, acquisition of the GAD insertion domain by bacterial AspRS might have facilitated GatCAB release from the Asn-transamidosome to better enable early bacteria to use GatCAB for both Gln-$tRNA^{Gln}$ and Asn-$tRNA^{Asn}$ formation. Consistent with this idea, the GAD insertion was likely acquired early on in bacterial AspRS evolution and coevolved for an extended time with the rest of the enzyme (*SI Text* and Fig. S8).

In *H. pylori*, Hp0100 stabilizes GatCAB association with bacterial ND-AspRS even in the absence of $tRNA^{Asn}$ (23). *H. pylori* also encodes two GluRS enzymes, with the second (GluRS2) complexing with GatCAB for Gln-$tRNA^{Gln}$ formation (31, 42, 43). Hp0100 and GluRS2 may be adaptations to better regulate the dual functions of *Hp*GatCAB. In *P. aeruginosa*, which acquired GlnRS and uses GatCAB for only Asn-$tRNA^{Asn}$ synthesis (25), retention of the GAD

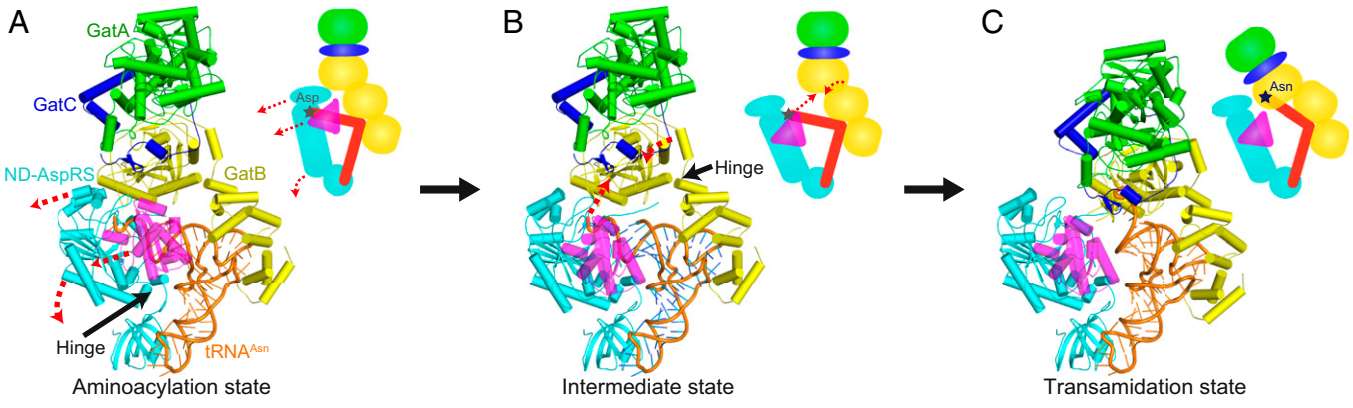

Fig. 6. Proposed reaction model for Asn-$tRNA^{Asn}$ synthesis in the bacterial Asn-transamidosome. Each component is color-coded as in Fig. 1. Aminoacylation (*A*), intermediate (*B*), and transamidation (*C*) states of the Asn-transamidosome are shown. Movement from the aminoacylation to the transamidation state is indicated by red dotted arrows. In the schematic diagram, the amino acid ligated to the $tRNA^{Asn}$ is represented by a star (Asp, gray; Asn, dark blue).

insertion in AspRS may be a remnant the coevolution of the protein domains in early bacteria. The insertion domain may still be selected for to allow proper folding of *Pa*ND-AspRS and to enable simultaneous activity of both monomers of ND-AspRS in the complex, thereby improving ND-AspRS turnover of $tRNA^{Asn}$. This coevolution may be preventing the generation of stable GAD domain deletion mutant *Pa*ND-AspRS enzymes.

Because the *Pa*Asn-transamidosome allows Asp-$tRNA^{Asn}$ to be directly handed off from ND-AspRS to GatCAB, the misaminoacylated tRNA is protected from deacylation and use in protein synthesis, where it may compromise the fidelity of translation. Accordingly, under certain conditions, the complex of ND-AspRS with GatCAB may be less prone than AsnRS to mischarged tRNA formation (8). In addition, the Asn-transamidosome allows *P. aeruginosa* to directly and efficiently couple the biosynthesis of Asn with its use in translation. As such, a similar complex between ND-AspRS and ancestral GatCAB pre-LUCAS might have enabled the addition of Asn to the genetic code (44).

Materials and Methods

Preparation of the *Pa*Asn-transamidosome and *Pa*ND-AspRS:$tRNA^{Asn}$ and the details of crystallization and structure determination are summarized in *SI Materials and Methods*. Structures of the *Pa*Asn-transamidosome and *Pa*ND-AspRS:$tRNA^{Asn}$ were solved by molecular replacement methods. Atomic coordinates and structure factors have been deposited in the Protein Data Bank under ID codes 4WJ3 for *Pa*Asn-transamidosome and 4WJ4 for *Pa*ND-AspRS:$tRNA^{Asn}$. Detailed descriptions of the gel-shift assay, gel filtration analysis, kinetic analysis, protection assay, and phylogenetic analysis using established methods are provided in *SI Materials and Methods*.

ACKNOWLEDGMENTS. We thank Dr. Keitaro Yamashita (RIKEN) and the beamline staff of BL41XU and BL44XU at SPring-8. We are grateful to Sergey Melnikov and Jiqiang Ling for their critical reading of the manuscript. This work was supported by a Grant-in-Aid for Scientific Research in a Priority Area (24567068, to M.Y.) and the Photon and Quantum Basic Research Coordinated Development Program (M.Y.) from the Ministry of Education, Culture, Sports, Science and Technology of Japan; a grant from the US National Science Foundation (MCB-1244326, to K.S.); and a grant from the National Institute of General Medical Sciences (GM22854, to D.S.). A.N. has received a Japan Society for the Promotion of Science Postdoctoral Fellow for Research Abroad.

1. Ibba M, Söll D (1999) Quality control mechanisms during translation. *Science* 286(5446): 1893–1897.
2. Ibba M, Söll D (2000) Aminoacyl-tRNA synthesis. *Annu Rev Biochem* 69:617–650.
3. Roy H, Becker HD, Reinbolt J, Kern D (2003) When contemporary aminoacyl-tRNA synthetases invent their cognate amino acid metabolism. *Proc Natl Acad Sci USA* 100(17):9837–9842.
4. Sheppard K, Akochy PM, Salazar JC, Söll D (2007) The *Helicobacter pylori* amidotransferase GatCAB is equally efficient in glutamine-dependent transamidation of Asp-$tRNA^{Asn}$ and Glu-$tRNA^{Gln}$. *J Biol Chem* 282(16):11866–11873.
5. Yuan J, Sheppard K, Söll D (2008) Amino acid modifications on tRNA. *Acta Biochim Biophys Sin (Shanghai)* 40(7):539–553.
6. Becker HD, Kern D (1998) *Thermus thermophilus*: A link in evolution of the tRNA-dependent amino acid amidation pathways. *Proc Natl Acad Sci USA* 95(22):12832–12837.
7. Cathopoulis T, Chuawong P, Hendrickson TL (2007) Novel tRNA aminoacylation mechanisms. *Mol Biosyst* 3(6):408–418.
8. Curnow AW, Ibba M, Söll D (1996) tRNA-dependent asparagine formation. *Nature* 382(6592):589–590.
9. Curnow AW, Tumbula DL, Pelaschier JT, Min B, Söll D (1998) Glutamyl-$tRNA^{Gln}$ amidotransferase in *Deinococcus radiodurans* may be confined to asparagine biosynthesis. *Proc Natl Acad Sci USA* 95(22):12838–12843.
10. Becker HD, et al. (2000) The heterotrimeric *Thermus thermophilus* Asp-$tRNA^{Asn}$ amidotransferase can also generate Gln-$tRNA^{Gln}$. *FEBS Lett* 476(3):140–144.
11. Salazar JC, et al. (2001) A dual-specific Glu-$tRNA^{Gln}$ and Asp-$tRNA^{Asn}$ amidotransferase is involved in decoding glutamine and asparagine codons in *Acidithiobacillus ferrooxidans*. *FEBS Lett* 500(3):129–131.
12. Raczniak G, Becker HD, Min B, Söll D (2001) A single amidotransferase forms asparaginyl-tRNA and glutaminyl-tRNA in *Chlamydia trachomatis*. *J Biol Chem* 276(49): 45862–45867.
13. Sheppard K, Sherrer RL, Söll D (2008) *Methanothermobacter thermautotrophicus* $tRNA^{Gln}$ confines the amidotransferase GatCAB to asparaginyl-$tRNA^{Asn}$ formation. *J Mol Biol* 377(3):845–853.
14. Lapointe J, Duplain L, Proulx M (1986) A single glutamyl-tRNA synthetase aminoacylates $tRNA^{Glu}$ and $tRNA^{Gln}$ in *Bacillus subtilis* and efficiently misacylates *Escherichia coli* $tRNA^{Gln1}$ *in vitro*. *J Bacteriol* 165(1):88–93.
15. Curnow AW, et al. (1997) Glu-$tRNA^{Gln}$ amidotransferase: A novel heterotrimeric enzyme required for correct decoding of glutamine codons during translation. *Proc Natl Acad Sci USA* 94(22):11819–11826.
16. Tumbula DL, Becker HD, Chang WZ, Söll D (2000) Domain-specific recruitment of amide amino acids for protein synthesis. *Nature* 407(6800):106–110.
17. Oshikane H, et al. (2006) Structural basis of RNA-dependent recruitment of glutamine to the genetic code. *Science* 312(5782):1950–1954.
18. Schön A, Kannangara CG, Gough S, Söll D (1988) Protein biosynthesis in organelles requires misaminoacylation of tRNA. *Nature* 331(6152):187–190.
19. Bailly M, Blaise M, Lorber B, Becker HD, Kern D (2007) The transamidosome: A dynamic ribonucleoprotein particle dedicated to prokaryotic tRNA-dependent asparagine biosynthesis. *Mol Cell* 28(2):228–239.
20. Bailly M, et al. (2008) tRNA-dependent asparagine formation in prokaryotes: Characterization, isolation and structural and functional analysis of a ribonucleoprotein particle generating Asn-$tRNA^{Asn}$. *Methods* 44(2):146–163.
21. Blaise M, et al. (2010) Crystal structure of a transfer-ribonucleoprotein particle that promotes asparagine formation. *EMBO J* 29(18):3118–3129.
22. Delarue M, et al. (1994) Crystal structure of a prokaryotic aspartyl tRNA-synthetase. *EMBO J* 13(14):3219–3229.
23. Silva GN, et al. (2013) A tRNA-independent mechanism for transamidosome assembly promotes aminoacyl-tRNA transamidation. *J Biol Chem* 288(6):3816–3822.
24. Fischer F, et al. (2012) The asparagine-transamidosome from *Helicobacter pylori:* A dual-kinetic mode in non-discriminating aspartyl-tRNA synthetase safeguards the genetic code. *Nucleic Acids Res* 40(11):4965–4976.
25. Akochy PM, Bernard D, Roy PH, Lapointe J (2004) Direct glutaminyl-tRNA biosynthesis and indirect asparaginyl-tRNA biosynthesis in *Pseudomonas aeruginosa* PAO1. *J Bacteriol* 186(3):767–776.
26. Bailly M, et al. (2006) A single tRNA base pair mediates bacterial tRNA-dependent biosynthesis of asparagine. *Nucleic Acids Res* 34(21):6083–6094.
27. Nakamura A, et al. (2010) Two distinct regions in *Staphylococcus aureus* GatCAB guarantee accurate tRNA recognition. *Nucleic Acids Res* 38(2):672–682.
28. Nakamura A, Yao M, Chimnaronk S, Sakai N, Tanaka I (2006) Ammonia channel couples glutaminase with transamidase reactions in GatCAB. *Science* 312(5782): 1954–1958.
29. Eiler S, Dock-Bregeon A, Moulinier L, Thierry JC, Moras D (1999) Synthesis of aspartyl-$tRNA^{Asp}$ in *Escherichia coli*—a snapshot of the second step. *EMBO J* 18(22):6532–6541.
30. Ito T, Yokoyama S (2010) Two enzymes bound to one transfer RNA assume alternative conformations for consecutive reactions. *Nature* 467(7315):612–616.
31. Huot JL, et al. (2011) Gln-$tRNA^{Gln}$ synthesis in a dynamic transamidosome from *Helicobacter pylori,* where GluRS2 hydrolyzes excess Glu-$tRNA^{Gln}$. *Nucleic Acids Res* 39(21):9306–9315.
32. Hausmann CD, Ibba M (2008) Aminoacyl-tRNA synthetase complexes: Molecular multitasking revealed. *FEMS Microbiol Rev* 32(4):705–721.
33. Hausmann CD, Praetorius-Ibba M, Ibba M (2007) An aminoacyl-tRNA synthetase: elongation factor complex for substrate channeling in archaeal translation. *Nucleic Acids Res* 35(18):6094–6102.
34. Godinic-Mikulcic V, Jaric J, Hausmann CD, Ibba M, Weygand-Durasevic I (2011) An archaeal tRNA-synthetase complex that enhances aminoacylation under extreme conditions. *J Biol Chem* 286(5):3396–3404.
35. Das M, Vargas-Rodriguez O, Goto Y, Suga H, Musier-Forsyth K (2014) Distinct tRNA recognition strategies used by a homologous family of editing domains prevent mistranslation. *Nucleic Acids Res* 42(6):3943–3953.
36. Srivastava DK, Bernhard SA (1986) Metabolite transfer via enzyme-enzyme complexes. *Science* 234(4780):1081–1086.
37. Bhaskaran H, Perona JJ (2011) Two-step aminoacylation of tRNA without channeling in Archaea. *J Mol Biol* 411(4):854–869.
38. Liu Y, et al. (2014) Ancient translation factor is essential for tRNA-dependent cysteine biosynthesis in methanogenic archaea. *Proc Natl Acad Sci USA* 111(29):10520–10525.
39. Yuan J, et al. (2010) Distinct genetic code expansion strategies for selenocysteine and pyrrolysine are reflected in different aminoacyl-tRNA formation systems. *FEBS Lett* 584(2):342–349.
40. Sheppard K, Söll D (2008) On the evolution of the tRNA-dependent amidotransferases, GatCAB and GatDE. *J Mol Biol* 377(3):831–844.
41. Becker HD, et al. (2000) *Thermus thermophilus* contains an eubacterial and an archaebacterial aspartyl-tRNA synthetase. *Biochemistry* 39(12):3216–3230.
42. Skouloubris S, Ribas de Pouplana L, De Reuse H, Hendrickson TL (2003) A noncognate aminoacyl-tRNA synthetase that may resolve a missing link in protein evolution. *Proc Natl Acad Sci USA* 100(20):11297–11302.
43. Salazar JC, et al. (2003) Coevolution of an aminoacyl-tRNA synthetase with its tRNA substrates. *Proc Natl Acad Sci USA* 100(24):13863–13868.
44. Sheppard K, et al. (2008) From one amino acid to another: tRNA-dependent amino acid biosynthesis. *Nucleic Acids Res* 36(6):1813–1825.